Springer Atmospheric Sciences

Darko Koračin
Clive E. Dorman *Editors*

Marine Fog: Challenges and Advancements in Observations, Modeling, and Forecasting

Springer

Springer Atmospheric Sciences

More information about this series at http://www.springer.com/series/10176

Darko Koračin • Clive E. Dorman
Editors

Marine Fog: Challenges and Advancements in Observations, Modeling, and Forecasting

Springer

Editors
Darko Koračin
Faculty of Science
Department of Physics
University of Split
Split, Croatia

Clive E. Dorman
Integrative Oceanography Division
Scripps Institution of Oceanography
University of California, San Diego
La Jolla, CA, USA

Department of Atmospheric Sciences
Desert Research Institute
Reno, NV, USA

Department of Geological Sciences
San Diego State University
San Diego, CA, USA

ISSN 2194-5217 ISSN 2194-5225 (electronic)
Springer Atmospheric Sciences
ISBN 978-3-319-45227-2 ISBN 978-3-319-45229-6 (eBook)
DOI 10.1007/978-3-319-45229-6

Library of Congress Control Number: 2016958809

Printed on acid-free paper

This Springer imprint is published by Springer Nature
The registered company is Springer International Publishing AG
The registered company address is: Gewerbestrasse 11, 6330 Cham, Switzerland

Contents

Contributors

Clive E. Dorman Integrative Oceanography Division, Scripps Institution of Oceanography, University of California, San Diego, La Jolla, CA, USA

Department of Geological Sciences, San Diego State University, San Diego, CA, USA

Jun Du NOAA/NCEP/Environmental Modeling Center, College Park, MD, USA

Ismail Gultepe Cloud Physics and Severe Weather Research, Environment and Climate Change Canada, Toronto, ON, Canada

Chang Ki Kim New and Renewable Energy Resource Center, Korea Institute of Energy Research, Daejeon, South Korea

Darko Koračin Faculty of Science, Department of Physics, University of Split, Split, Croatia

Department of Atmospheric Sciences, Desert Research Institute, Reno, NV, USA

John M. Lewis National Severe Storms Laboratory, Norman, OK, USA

Desert Research Institute, Reno, NV, USA

Daniel McEvoy Western Regional Climate Center, Desert Research Institute, Reno, NV, USA

John Mejia Department of Atmospheric Sciences, Desert Research Institute, Reno, NV, USA

Jason A. Milbrandt Atmospheric Numerical Weather Prediction Research, Environment and Climate Change Canada, Dorval, QC, Canada

Robert Tardif Department of Atmospheric Sciences, University of Washington, Seattle, WA, USA

Eric M. Wilcox Division of Atmospheric Sciences, Desert Research Institute, Reno, NV, USA

Seong Soo Yum Department of Atmospheric Sciences, Yonsei University, Seoul, South Korea

Suping Zhang Key Laboratory of Physical Oceanography & Ocean-Atmosphere Interaction and Climate Laboratory, Ocean University of China, Qingdao, China

Binbin Zhou I. M. Systems Group and NOAA/NCEP/Environmental Modeling Center, College Park, MD, USA

Chapter 1
Introduction

Darko Koračin and Clive E. Dorman

Abstract Marine fog has a significant impact on human activities and the environment. A substantial portions of all accidents at sea worldwide occur in the presence of dense fog. Fog's disruption of marine transport, harbor activities, coastal road traffic, and life threatening situations are often in the news. Fog transports droplets and their ions, aerosols, and microorganisms that alter the hydrologic, thermodynamic, nutrient, and toxicological properties of ecosystems in coastal regions. Fog also controls temperature and moisture conditions in coastal areas and consequently affects vegetation and especially forest evolution. Some of the highest degradations of air quality occur during fog under stable and stagnant anticyclonic conditions. In principle, fog forecast models should resolve a huge span of physical processes ranging from the characteristic 10^{-7} m scales of aerosols to synoptic processes with scales of 10^{6} m, which means the range of the smallest to the largest scales is on an order of 10^{13} m. The main variables and processes relevant to fog include aerosols and fog condensation nuclei; microphysics and precipitation; advection; synoptic conditions; air-sea interaction through surface fluxes of heat, latent heat, moisture, and momentum; air and sea surface temperature; ocean currents and upwelling; land-sea interactions and local circulations; characteristics of low marine inversion and entrainment; and coastal topography. The main goal of this book is to provide comprehensive understanding of the major processes leading to formation, evolution, and dissipation of fog by using observations, modeling, and forecasting. Discussed topics include fog observational in situ

D. Koračin (✉)
Faculty of Science, Department of Physics, University of Split, Ruđera Boškovića 33, 21000 Split, Croatia

Department of Atmospheric Sciences, Desert Research Institute, 2215 Raggio Parkway, Reno, NV 89512, USA
e-mail: dkoracin@pmfst.hr; Darko.Koracin@dri.edu

C.E. Dorman
Integrative Oceanography Division, Scripps Institution of Oceanography, University of California, San Diego, 9500 Gilman Drive # 0209, La Jolla, CA 92093-0209, USA

Department of Geological Sciences, San Diego State University, 5500 Campanile Drive, San Diego, CA 92182-1020, USA
e-mail: cdorman@ucsd.edu

D. Koračin, C.E. Dorman (eds.), *Marine Fog: Challenges and Advancements in Observations, Modeling, and Forecasting*, Springer Atmospheric Sciences,
DOI 10.1007/978-3-319-45229-6_1

and remote sensing techniques, worldwide fog climatology, radiation and turbulence properties, microphysics and visibility parameterizations, effects of precipitation on fog, and deterministic and probabilistic fog modeling and forecasting.

In general, fog is a phenomenon that we all experience in our lives and impacts our activities and the environment. When we wish to discuss marine fog, the first step is to review the definition of fog. We can start with the definition from the Glossary of the American Meteorological Society (http://glossary.ametsoc.org): "Fog is a hydrometeor consisting of a visible aggregate of minute water droplets suspended in the atmosphere near the earth's surface. According to international definitions, fog reduces visibility below 1 km (0.62 miles). Fog differs from cloud only in that the base of fog is at the earth's surface while cloud bases are above the surface." According to the Glossary, the main mechanism for fog formation is: "Fogs of all types originate when the temperature and dew point of the air become identical (or nearly so), provided that sufficient condensation nuclei are available. This may occur either through cooling of the air to its dew point (producing advection fog, radiation fog, or upslope fog), or by adding moisture and thereby elevating the dew point (producing steam fog or frontal fog). Fog seldom forms when the dew-point spread is greater than 4 °F." The Glossary also explains fog subsets and differences among fog, haze and mist. "According to U.S. weather observing practice, fog that hides less than 0.6 of the sky is called ground fog. If fog is so shallow that it is not an obstruction to vision at a height of 6 ft above the surface, it is called simply shallow fog. Fog is easily distinguished from haze by its higher relative humidity (near 100 %, having physiologically appreciable dampness) and gray color. Haze does not contain activated droplets larger than the critical size according to the Köhler theory. Mist may be considered an intermediate between fog and haze; its particles are smaller (a few μm maximum) in size, it has lower relative humidity than fog, and does not obstruct visibility to the same extent."

While considering the many books on bookstore shelves and information available throughout the media, a reader might ask an appropriate question: Why a book on marine fog? Also, more precisely, why focus on marine fog? The oceans cover 71 % of the earth's surface and contain 97 % of the water on the earth's surface; however, due to abundant measurements over the land compared to over the ocean, land fog is much more investigated than to sea fog. Additionally, it should be noticed that most large world cities are located in coastal regions. Due to a lack of routine measurements at fixed locations over vast portions of the ocean, measurements and predictions of sea fog represent a great challenge for research and application studies. Because of the air-sea-land interaction processes, sea fog can be advected to land and appear as coastal land fog and vice versa. An indirect effect can also occur when aerosols originating from the land are transported over the sea and initiate sea fog. Even simple advection of the moisture during sea breezes and onshore flows can provide enough moisture for nighttime radiative cooling and fog formation over land. Consequently, fogs over the coastal sea and land can be mutually connected and we call this joint phenomenon marine fog.

Fog, and marine fog in particular, make a significant impact on human activities and the environment. Significant number of cases of all accidents at sea worldwide occur in the presence of dense fog. Fog disrupts marine transport, harbor activities, coastal road traffic, and causes life threatening situations. At some airports there are efforts to artificially dissipate fog by inducing mixing and turbulence with ventilation systems, aerosol and ice seeding, and warming systems to evaporate fog droplets. Fog also makes significant impact on ecology by transporting water and organic and inorganic substances onto coastal ecosystems. The transported droplets and their ions, aerosols, and microorganisms alter the hydrologic, thermodynamic, nutrient, and toxicological properties of ecosystems in coastal regions. Fog alters temperature and moisture conditions in coastal areas. Sea fog can drift and transport aerosols and water onto coastal land and together with the fog originating over the land can change environmental conditions. Fog significantly affects vegetation, especially forest evolution in coastal areas. Future projections of declining fog frequency in some areas will also induce declines in certain species of coastal vegetation and a consequent impact on animals. Some of the highest degradations of air quality occur during fog under stable and stagnant anticyclonic conditions. This frequently happens in industrial areas where fog is mixed with locally generated pollution to form a combination known as smog.

Besides negative impacts due to fatalities and damages, there are positive aspects of marine fog in areas with low hydrology reserves—fog collecting becomes an important source of increasing water supply. In coastal regions, fog supplies moisture for the evolution of forests. From some viewpoints, fog provides an enjoyable aesthetic view, and has been inspiration and background for literature and movies.

Fog is elusive with great spatial and temporal variability, which makes it extremely difficult to describe quantitatively and yet even more difficult to accurately predict on synoptic and climate scales. Fog forecasting has a long history. Generally, people connected fog appearance with good and stable weather. Prior to and during WWII, operational weather forecasting centers were using analysis of weather observations and providing forecasts based on statistical and empirical methods, but also using experience and intuition. After WWII, with the establishment of weather communication systems and an expanded measurement network, weather forecasting has undergone major developments. A major development was the advent of computer systems and numerical weather forecasting models in the second part of the twentieth century.

In principle, forecast models should resolve a huge span of physical processes ranging from the characteristic 10^{-7} m scales of aerosols to synoptic processes with scales of 10^{6} m, which means the range of the smallest to the largest scales is on an order of 10^{13} m. The main parameters and processes relevant to fog include aerosols and fog condensation nuclei; microphysics and precipitation; advection; synoptic conditions; air-sea interaction through surface fluxes of heat, latent heat, and momentum; sea surface temperature; ocean currents and upwelling/downwelling; land-sea interactions and local circulations; characteristics of low—level marine inversion and entrainment; and coastal topography. All of these scales and

processes impose great difficulty on numerical prediction. Global models are too coarse to resolve a full scale of fog processes, but regional and mesoscale models are generally able to reproduce and predict synoptic processes. Fog measurements are mainly conducted over the land while sea fog over the oceans lacks routine and fixed measurements and networks to cover it. Satellite detection, data analysis, and interpretation are emerging tools with great potential for determining the worldwide spatial and temporal properties of fog, but still with significant problems related to detection algorithms not fully resolving fog layers. Specifically, fog layers are usually only a few hundred meters deep, so that the fog top temperatures are close to the local sea surface temperatures. Consequently, satellite detection algorithms are not always able to fully differentiate fog layers from the surrounding sea. Standard worldwide fog climatology extends about to the 1950s at sea and perhaps to the 1930s on land. However, with the rapid expansion of sea traffic after 1950 and installation of buoy networks after 1980, there is now a large data base for climate studies that has been explored in this book.

Another important question is the role of fog in scenarios of climate change. Due to their high albedo and persistence in many areas of the world, fog layers represent a notable component of the air-earth-ocean radiation balance. Future fog properties including frequency, intensity, and spatial changes will influence climate evolution. However, global climate models with coarse resolutions and limited physics parameterizations cannot resolve the finer scales of fog necessary to determine details of the physical processes relevant to fog formation, evolution, and dissipation. Regional climate models with resolutions on the order of several tens of kilometers or better are improved tools, but are still not able to accurately resolve or predict all fog phases. Note that initial and boundary conditions for regional climate models are still derived from the global climate models for the future projections and for historical simulations. Details of fog projections in climate change scenarios are important and relevant to planning future activities in many areas including traffic, energy, fisheries, agriculture, hydrology, and forestry.

There is a definite need to enhance sea-based observational networks including buoys and ships and improve satellite fog retrievals as well as spatial and temporal resolution of data. Intensive field programs are needed to understand details of fog 3D structure and evolution on all scales from aerosols and fog condensation nuclei to synoptic scales. Modeling and forecasting need to achieve higher accuracy of fog predictions, despite current insufficient resolution and inaccurate representation of physical processes as well as inaccurate initial and boundary conditions. Statistical methods, including those based on principles of artificial intelligence, are valuable tools in operational forecasting for a particular location, but they cannot provide results under conditions of significant synoptic evolution. Coupling high-resolution one-dimensional models with relatively coarse-resolution 3D models has been yielding better results than 3D models alone. Some advanced numerical techniques such as large-eddy simulations have been applied to fog prediction and show promise in approaching the fine scales of fog processes. Full coupling between atmospheric and ocean models will need to be considered for predicting marine fog. Significant advances in fog predictions are provided by ensemble forecasting,

which reveals model uncertainty and introduces probabilistic forecasts of fog. Studies also show that understanding air-mass pathway history can be crucial to determining and predicting fog characteristics. Some studies show that, in addition to all forecasting techniques, a subjective insight from an experienced forecaster can improve the final fog forecast in many cases. Although fog predictions represent a significant challenge to climate modeling, the use of future-developed, high-resolution climate models is essential to estimating projections of fog properties and distributions, which are extremely important to understanding the evolution of fog impacts on human activities and ecosystems.

The structure of the book by chapters is as follows.

Chapter 2. Worldwide Marine Fog Occurrence and Climatology

An analysis of marine weather observations collected from 1950–2007 as part of the International Comprehensive Ocean-atmosphere Data Set (ICOAD) has resulted in a unique climatology of marine fog, shallow fog, and mist.

Chapter 3. Early and Recent Observational Techniques for Fog

The observational techniques from the early 1950s to date for fog and related atmospheric parameters as well as for lower atmospheric boundary layer are examined including data examples.

Chapter 4. Turbulence in Marine Fog

The roles of the turbulent transport of heat and moisture in the marine environment from both observational and modeling studies are examined to explain the importance of turbulence in marine fog formation.

Chapter 5. Radiation in Marine Fog

The chapter elaborates on the role of longwave and shortwave radiation transfers and complexities of their parameterizations on the formation and evolution of marine fog.

Chapter 6. Synoptic Processes

The chapter presents importance of synoptic processes and seasonal variability on the formation, evolution, and dissipation of marine fog along the Chinese coast and Yellow Sea where the deepest marine fogs in the world occur.

Chapter 7. A Review on Microphysics and Visibility Prediction

The areas of marine fog related research and operations that are discussed in the chapter include aspects of visibility, microphysical parameters such as liquid water content, aerosol particle size distribution, nucleation, drop size distribution, degree of supersaturation, radiation and particle interaction, heat and moisture fluxes, and dynamics of the system at various scales.

Chapter 8. Precipitation and Fog

Building on early as well as more recent studies, this chapter presents a comprehensive description of our current level of understanding of key physical principles involved in the formation and evolution of precipitation fog—a lesser known yet important aspect of the fog phenomenon.

Chapter 9. Modeling and Forecasting of Marine Fog

Historical review and analysis of various fog modeling and forecasting techniques using statistical and dynamical models as well as challenges in model development and applications to various regions worldwide is discussed in this chapter.

Chapter 10. Ensemble Fog Prediction

The chapter presents new advances in fog research by using probabilistic forecasting and estimating uncertainties related to models and input data.

Chapter 11. Multi-spectral Remote Sensing of Sea Fog with Simultaneous Passive Infrared and Microwave Sensors

This chapter uses a combination of the satellite standard visible/infrared data combined with a co-located retrieval of sea surface temperature from microwave imager data to remotely detect marine fog.

Chapter 2
Worldwide Marine Fog Occurrence and Climatology

Clive E. Dorman, John Mejia, Darko Koračin, and Daniel McEvoy

Abstract Herein, an analysis is presented of the world's marine fog distribution based upon the International Comprehensive Ocean-atmosphere Data Set (ICOADS) ship observations taken during 1950–2007. Fog, shallow fog, and mist are taken from routine weather reports that are encoded in an ICOADS ship observation with the "present weather" code. Occurrence is estimated by the number of observations of a type divided by the total present weather observations in a one-degree area. The bulk of the observations are in the northern temperate and tropical oceans, with decreasing numbers south of 20 °S and large data voids in the polar oceans. Marine fog is infrequent over most of the world's oceans with the median occurrence 0.2 % while it is in isolated maxima for values larger than about 2 %. In a specific location, either fog or mist are the most frequent, followed with an order of magnitude lower occurrence by shallow fog.

The two major open ocean fog maxima in the world occur on the northwestern side of northern hemisphere oceans during the summer under atmospheric subsidence

C.E. Dorman (✉)
Integrative Oceanography Division, Scripps Institution of Oceanography, University of California, San Diego, 9500 Gilman Drive # 0209, La Jolla, CA 92093-0209, USA

Department of Geological Sciences, San Diego State University, 5500 Campanile Drive, San Diego, CA 92182-1020, USA
e-mail: cdorman@ucsd.edu; cdorman@mail.sdsu.edu

J. Mejia
Department of Atmospheric Sciences, Desert Research Institute, Reno, NV 89512, USA
e-mail: john.mejia@dri.edu

D. Koračin
Faculty of Science, Department of Physics, University of Split, Ruđera Boškovića 33, 21000 Split, Croatia

Department of Atmospheric Sciences, Desert Research Institute, 2215 Raggio Parkway, Reno, NV 89512, USA
e-mail: dkoracin@pmfst.hr; Darko.Koracin@dri.edu

D. McEvoy
Western Regional Climate Center, Desert Research Institute, Reno, NV 89512, USA
e-mail: Daniel.McEvoy@dri.edu

D. Koračin, C.E. Dorman (eds.), *Marine Fog: Challenges and Advancements in Observations, Modeling, and Forecasting*, Springer Atmospheric Sciences,
DOI 10.1007/978-3-319-45229-6_2

over a cold polar current. The distribution of the center of the maximum and highest values are over shallow water and follow the shape of the shallow bathymetry. For the highest occurrences, surface air is preconditioned by warming over a western boundary current followed by cooling over a negative SST gradient and stable lower atmosphere suppressing boundary layer exchange with the air above. The horizontal fog structure is set by surface ocean currents, sea surface temperature gradients and seasonal wind direction. Marine fog's most frequent occurrence and largest areal coverage is in the NW Pacific in June–July–August, reaching its peak value of 59.8 % over the Kuril Islands on the western side of the Ohyashio current. The second largest marine fog maximum occurrence is in the NW Atlantic in June–July–August, reaching 45.0 % over the Grand Banks and the Labrador Current. The eastward extent of both of the NW ocean maxima is determined by the sub-polar ocean gyre.

Wind driven coastal ocean upwelling regions have a narrow zone of fog located against the coast, over the inner shelf and over the sea surface temperature minimum along the coast. A mist maximum occurs in a broader area beyond the temperature minimum. The lowest fog occurrence is in the cold season and the highest is in the warm season for all five areas except SW Africa which has its maximum in March–April–May. SW Africa has the highest single grid point fog occurrence and its upwelling, which lasts all year, and fog maximum, are both divided into two, separate areas. California–Oregon has the greatest along coast extent of fog occurrence and SST minimum as well at the lowest SST minimum. NW Africa, and Peru have significantly less fog occurrence, a shorter extent along coast of fog and a higher minimum SST. For all of the wind driven coastal upwelling zones, the Arabian Peninsula has the least fog occurrence, the shortest along coast extent as well as the highest SST minimum.

Significant fog and mist occurs at mid-latitudes in marginal seas and along the western side of northern hemisphere oceans. Over the NW Pacific, fog occurrence average of the 5 highest grid point values in the Sea of Okhotsk is 51 % in June–July–August, in the Japan Sea it is 27 % in June–July–August and the Yellow Sea it nears 15 % during March–April–May and June–July–August. The greatest fog and mist occurs along the southern China coast in December–January–March and March–April–May when the average of the 5 highest values are between 4 % and 6 %. On the NW Atlantic along the NE United States and Canada fog is most prevalent in June–July–August and least in December–January–February. During June–July–August, an elevated fog occurrence over the shelf extends along the coast from Cape Cod to SW Labrador that includes a maximum centered off the SE tip of Nova Scotia where the average of the five highest fog grid point occurrences is 41 %. The Nova Scotia maximum center is separate from that over the Grand Banks.

On the NE Atlantic appreciable fog and mist occurs around the N. European coastline in all seasons. In the North Sea, the average of the fog 5 highest grid point occurrences is greatest in March–April–May (8 %) and least in September–October–November (4 %). For the Baltic Sea, the average of the five highest fog grid point occurrences is most in March–April–May (15 %), and least is in September–October–November (6 %).

The polar seas have their greatest fog and mist occurrences during the warm season and the least during the cold season. The transitional seasons appear to have

intermediate fog and mist values around the periphery while the interior is largely unsampled. Observations are mostly limited to the warm season, distributed unevenly and with vast areal data voids.

There are significant fog occurrence climate trend increases tested at the 0.05 significance level for June–July–August based upon the 1950–2007 record in three areas with high numbers of ship observations. The open ocean Kuril Island maximum occurrence in NW Pacific increased by 15.8 % and the Grand Banks maximum in the NW Atlantic increased by 12.8 %. The sea surface temperature (SST) over the same area and same period also increased which is consistent with published SST increases in the adjacent western boundary currents in both oceans. The third case is the increase of 7.4 % of the fog occurrence maximum along the California–Oregon coast over wind driven upwelling water. In contrast to the NW Ocean maximums, this coastal fog maximum is associated with a long term SST decrease.

1 Introduction

The collection and retention of marine data in the late nineteenth and early twentieth century were greatly expanded by the interest that was initially focused on land. Foremost among these was the International Meteorological Organization (Sarukhanian & Walker n. d.). In 1923, the IMO passed a resolution that resulted in data captured from hundreds of stations around the world (World Meteorological Organization, n. d. a). The collection of meteorological data on a worldwide scale was further encouraged by and organized with conferences after WWII. In 1951, the IMO formally became the World Meteorological Organization (WMO), an agency of the United Nations, in direct succession from the IMO.

With the international interest came the development and acceptance of the surface synoptic observations (SYNOP) meteorological reporting code, with defined procedures and protocols for taking and encoding weather observations. This step was crucial for worldwide ocean coverage due to the multinational aspect of ships. Developed in the late 1940/1950s, this program evolved in the United States to become the Federal Meteorological Handbook No. 1—Surface Weather Observations and Reports (FMH-1, 2005) and FM-12 by the WMO. The international collection and retention of weather SYNOP observations is encouraged by the Voluntary Observing Ship (VOS) scheme through the WMO (World Meteorological Organization, n.d. b) and by many countries (http://www.vos.noaa.gov/vos_scheme.shtml). The adoption of the SYNOP code for observations greatly increased the standardization of recording atmospheric conditions, reducing ambiguities and making subtle differences and trends more detectable over time and areas that are crucial not only to climate, but also to synoptic scale studies.

A special focus agency to assemble global surface marine data from the late seventeenth century to date began in 1981, as initial archiving of this data in the

United States was as the Comprehensive Ocean-atmosphere Data Set (COADS). The formal designation was changed to International COADS (ICOADS) to recognize the multinational input into the blended observational database and other benefits gained from extensive international collaboration (Slutz et al., 1985, http://weather.unisys.com/wxp/Appendices/Formats/SYNOP.html). A list of publications is available at http://icoads.noaa.gov/publications.htm. ICOADS is the principle source of observations used in this study.

2 Present Weather Observations Over the Sea

2.1 Data Source

Most of the data used in the present analysis is based on global ship weather observations from ICOADS, which was introduced in the previous section. The data used are from 1950 through 2007, from Release 2.5, Individual Observations, ds 540.0, Release 2.5.1 Intermediate, in experimental-2 format at http://rda.ucar.edu/datasets/ds540.0/#!access. The data is organized by individual ship observations, by month and year for the world, in the IMMA format described in http://rda.ucar.edu/datasets/ds540.0/index.html#!docs and discussed in Woodruff, Slutz, Jenne, and Steurer (1987), Worley, Woodruff, Reynolds, Lubker, and Lott (2005), and Woodruff, Diaz, Worley, Reynolds, and Lubker (2005). The majority of the modern data since the mid-1900s is ship data that was taken in the SYNOP format.

The question of quality arises when dealing with marine data taken under a range of circumstances, observer experience, and technological and institutional changes, not to mention the alteration of observing practices and weather codes that have occurred since the mid-1900s. Additional complications are that a significant amount of data is incomplete or has observational or encoding errors. The ICOADS agency publications document past quality control actions that were taken in an attempt to correct obvious errors. A relatively recent action was to eliminate duplicates, a nontrivial exercise when millions of observations can arrive at an archive through different pathways. Another step is to compare objective measurements with climatology and to flag outliers. The experience of the authors of this chapter is that the bulk of the observations are consistent and are useful for climate studies.

2.2 Methodology for the Fog Event Data Base

This study focuses almost exclusively on ICOADS "present weather," which characterizes the weather at the moment of observation and during the previous hour. This is an observer's subjective assessment based on looking around outside,

Table 2.1 Present weather codes related to fog

ww Code	Weather	Qualification
ww = 00–49 No precipitation at the station at the time of observation		
ww = 00–19 No precipitation, fog, ice fog (except for 11 and 12), dust storm, sandstorm, or drifting or blowing snow at the station at the time of observation or, except for 09 and 17, during the preceding hour		
ww = 04–09 Haze, dust, sand, or smoke		
10	Mist	
11	Patches	11–12, shallow fog or ice fog at the station, whether on land or sea, not deeper than about 2 m on land or 10 meters at sea
12	More or less continuous	
ww = 20–29 Precipitation, fog, ice fog, or thunderstorm at the station during the preceding hour, but not at the time of observation		
28	Fog or ice fog	During the preceding hour, but not at the time of observation
ww = 30–39 Dust storm, sandstorm, or drifting or blowing snow		
ww = 40–49 Fog or ice fog at the time of observation		
40	Fog or ice fog at a distance at the time of observation, but not at the station during the preceding hour; the fog or ice fog extending to a level above that of the observer	
41	Fog or ice fog in patches	
42	Fog or ice fog, sky visible	42–43 has become thinner during the preceding hour
43	Fog or ice fog, sky invisible	
44	Fog or ice fog, sky visible	44–45 no appreciable change during the preceding hour
45	Fog or ice fog, sky invisible	
46	Fog or ice fog, sky visible	46–47 has begun to or has become thicker during the preceding hour
47	Fog or ice fog, sky invisible	
48	Fog, depositing rime, sky visible	
49	Fog, depositing rime, sky invisible	
ww = 50–59 Drizzle		
ww = 60–69 Rain		
ww = 70–79 Solid precipitation, not in showers		
ww = 80–99 Showery precipitation or precipitation with current or recent thunderstorm		

Adapted from Woodruff et al. (1987)
Those used in this study are bold

checking measurements, and then assigning a two-digit code from 01 to 99, according to the SYNOP code. Codes that are or might be related to fog are listed in Table 2.1. The primary fog conditions are expressed by codes 40–49, which specify fog as a cloud deeper than 10 m touching the Earth's surface with the horizontal visibility less than or equal to 1 km. We consider these as descriptions as representative of fog for purposes of this study, and distinguish them from shallow fog. Codes 11 and 12 designate the occurrence of "shallow fog or ice fog at the

station, not deeper than about 10 m at sea." Shallow fog does not envelop the observer on most reporting vessels and does not expressly meet the restricted visibility criterion for the conventional definition of fog. Mist (code 10), might be considered a sort of near fog condition wherein water droplets restrict visibility in the surface layer, but not less than 1 km, and it does not meet the visibility limit for fog. We do not include Code 28, "fog or ice fog," which "occurred during the preceding hour but not at time of observation," as it does not occur at the time of observation, over weights the occurrence of fog when compared to those which occur at the time of observation and is a more ambiguous characterization that is not necessarily accompanied with visibility or other supporting meteorological data. Haze (05) is excluded, as it is generally includes factors other than water droplets such as dust, smoke, and has a different color, droplet diameter distribution and a greater visibility than fog.

We should mention two other observations related to fog that are not included in this analysis. One observation is "past weather," a single-digit element of the original SYNOP code absorbed into the ICOADS observation in 1982. Code #4 of this element is for "fog or ice fog or thick haze" during the past hour. This condition is not counted as fog in this study, as this aspect is not present at the time of observation, it assigns a different meaning to fog than what is used for fog, and it mixes haze and fog. The other observation is "total cloud amount (cover)," also represented by a single digit. The intent of this element is for the observer to estimate, subjectively, the amount of cloud covering the sky, ranging from clear (no cloud, coded 0) through 1/8 steps to totally covered (8/8, coded 8). The situation was coded as 9 if the observer could not see or distinguish what was above, characterized as "sky obscured by fog and/or other meteorological phenomena." This condition is not counted as fog, due to the ambiguous nature of this element that mixes fog and "other," such as precipitation and mist. This observation can be even more ambiguous on a dark night, when an observer is reduced to assuming cloud cover if stars cannot be seen and has to guess whether it is due to cloud or if the sky is obscured by something else. Finally, there were additional discussions regarding total cloud amount in the ICOADS documentation that are not repeated here.

2.3 Percent of Occurrence and Adjustment

Between January 1983 and February 1985, not reporting the present weather code was allowed if there was no significant weather. For 26 months, if there was no present weather reported, it could be that the present weather was not observed or that the weather was observed but it was not significant (WMO, 1994). This practice biased the count of a weather type toward the high side. To correct this situation, if the present weather code was missing for the period January 1983–February 1985, then the total cloud cover was examined, and if a code of 0–8 was reported, the sky was considered observable and there could not have been fog. In this case, the count

of total number of present weather observations is increased by one. During this period, the median ratio of the number of observations missing present weather but with a total cloud cover entry to the total number of observations was 0.26. By comparison, this ratio was much lower during the summers of the 1970s when this ratio was only 0.02.

We follow the practice by others who report fog as a percent of occurrence. In this chapter, the percent of observations for a weather type (such as fog, shallow fog, mist) is the sum of all applicable occurrences in that category divided by the sum of all present weather code occurrences then multiplied by 100.

2.4 Data Base Specifics: Reporting Codes

The data period begins in 1950 and ends in 2007, which was the most recent data available when this investigation initiated. The start date was chosen as it is near the initial development and adoption of the SYNOP format, with its formalized weather codes or its predecessor, as well as the dramatic increase in the number of ship observations after WWII. Although the ICOADS ship observations reach back into the age of sail on account of digitization of hand written ship logs, the number of ship observations falls off sharply before about 1950 and there are many limitations to their usefulness to due to the lack of standardization. In this analysis, the minimum resolution of observations is one-degree grid points over the oceans by 3 month season and year. The median percent of fog occurrence for the world for the data period is low, 0.2 %, and the standard deviation is 8 %. After examining the ICOADS data, it appears that 100 is the minimum number of observations required to compute a stable fog occurrence at a grid point for a season. The bulk of the present weather observations is in the north and central Pacific and Atlantic oceans while there are great gaps and little coverage south of the tropics as well the Polar Regions.

2.5 Frequency Distribution of the Weather Codes in the Data Base

We examine the distribution of the present weather observations for the world's oceans over the 1950–2007 period to give an impression about the relative frequency of occurrence. The numbers and ranks of selected codes that are fog designated, possibly related to fog, or have large numbers of observations are shown in Table 2.2 for JJA and Table 2.2 for DJF. All codes numbers for JJA are shown in Fig. 2.1a, with the smallest being a few hundred. In JJA, the first four codes, 00–03, make up the bulk of observations with 75 % of the total. Fog observations (40–49) make up 5.2 % of the observations, with code 45 being the

Table 2.2 Worldwide distribution of some ICOADS Present Weather Code (ww) observations 1950–2007 (though majority are in northern hemisphere)

ww code	Rank	Number of Obs $\times 10^3$	Weather condition
(a) During June–July–August			
00	4	1641	Cloud development not observed
01	2	3871	Clouds generally dissolving
02	1	13,322	State of sky on the whole unchanged
03	3	3564	Clouds generally forming or developing
04	39	23	Visibility reduced by smoke, forest fires, industrial smoke, or volcanic ash
05	8	612	Haze
10	7	659	Mist
11	33	51	Patches, low fog <10 m
12	32	55	Continuous, low fog <10 m
28	25	112	Past hour, not at observation time, fog
40	27	96	Fog at a distance, level above the observer
41	26	100	Fog or ice fog in patches
42	28	78	Fog or ice fog, sky visible, becoming thinner
43	25	111	Fog or ice fog, sky invisible, becoming thinner
44	21	149	Fog or ice fog, sky visible, no change in past hour
45	5	754	Fog or ice fog, sky invisible, no change in past hour
46	30	65	Fog or ice fog, sky visible, becoming thicker in preceding hour
47	16	200	Fog or ice fog, sky invisible, becoming thicker in preceding hour
48	60	5	Fog, depositing rime, sky visible
49	47	16	Fog, depositing rime, sky invisible
Blocks			
00–03		22,398	Four most frequent observations
04–09		4254	Haze, dust, sand, or smoke
20–29		1022	Precipitation, fog, ice fog, or thunderstorm at the station during the preceding hour but not at time of observation
30–39		42	Dust storm, sandstorm, or drifting or blowing snow
40–49		1575	Fog
50–59		699	Drizzle
60–69		946	Rain
70–79		25	Solid precipitation (snow) not in showers
80–99		563	Showers or recent thunderstorm
(b) During December–January–February			
00	4	1587	Cloud development not observed
01	2	3803	Clouds generally dissolving
02	1	12,359	State of sky on the whole unchanged
03	3	3499	Clouds generally forming or developing
04	58	14	Visibility reduced by smoke, forest fires, industrial smoke, or volcanic ash

(continued)

Table 2.2 (continued)

ww code	Rank	Number of Obs $\times 10^3$	Weather condition
05	11	255	Haze
10	8	304	Mist
11	49	22	Patches, low fog <10 m
12	47	23	Continuous, low fog <10 m
40	50	22	Fog at a distance, level above the observer
41	45	24	Fog or ice fog in patches
42	56	16	Fog or ice fog, sky visible, becoming thinner
43	55	19	Fog or ice fog, sky invisible, becoming thinner
44	40	31	Fog or ice fog, sky visible, no change in past hour
45	26	93	Fog or ice fog, sky invisible, no change in past hour
46	61	13	Fog or ice fog, sky visible, becoming thicker, preceding hour
47	41	31	Fog or ice fog, sky invisible, becoming thicker, preceding hour
48	87	3	Fog, depositing rime, sky visible
49	77	4	Fog, depositing rime, sky invisible
Blocks			
00–03		21,248	Four most frequent observations
04–09		361	Haze, dust, sand, or smoke
20–29		1264	Precipitation, fog, ice fog, or thunderstorm at the station during the preceding hour but not at time of observation
30–39		27	Dust storm, sandstorm, or drifting or blowing snow
40–49		256	Fog
50–59		562	Drizzle
60–69		1045	Rain
70–79		495	Solid precipitation (snow) not in showers
80–99		875	Showers or recent thunderstorm

fifth most frequent ww observation. Mist, code 10, is ranked seventh while shallow fog, codes 11 and 12, are ranked 32 and 33 which is low compared to fog or mist. Also noted in Table 2.2 and Fig. 2.1a, b are the number of observations for the weather type blocks of codes for drizzle, rain, snow, and showers (rain and thunder), which are observed less frequently than fog.

Continuing with the ww codes, we examine the December, January, and February (DJF) distribution for 1950–2007, to contrast with that in JJA. In this period, there were a similar number of present weather observations (Table 2.2). All codes numbers are shown in Fig. 2.1b, with the smallest being a few hundred. Again, the first four codes make up the bulk of the observations, with 77 %. The fog observations (40–49) are reduced to 0.9 % of the observations, with code 45, the most frequent fog observation, reduced to the rank of 26th in observation frequency. As most of the observations are in the northern hemisphere, snow (70s) and showers (80s and 90s) have increased considerably from JJA, but they remain a small portion of the season total. Rain observations are about the same, while

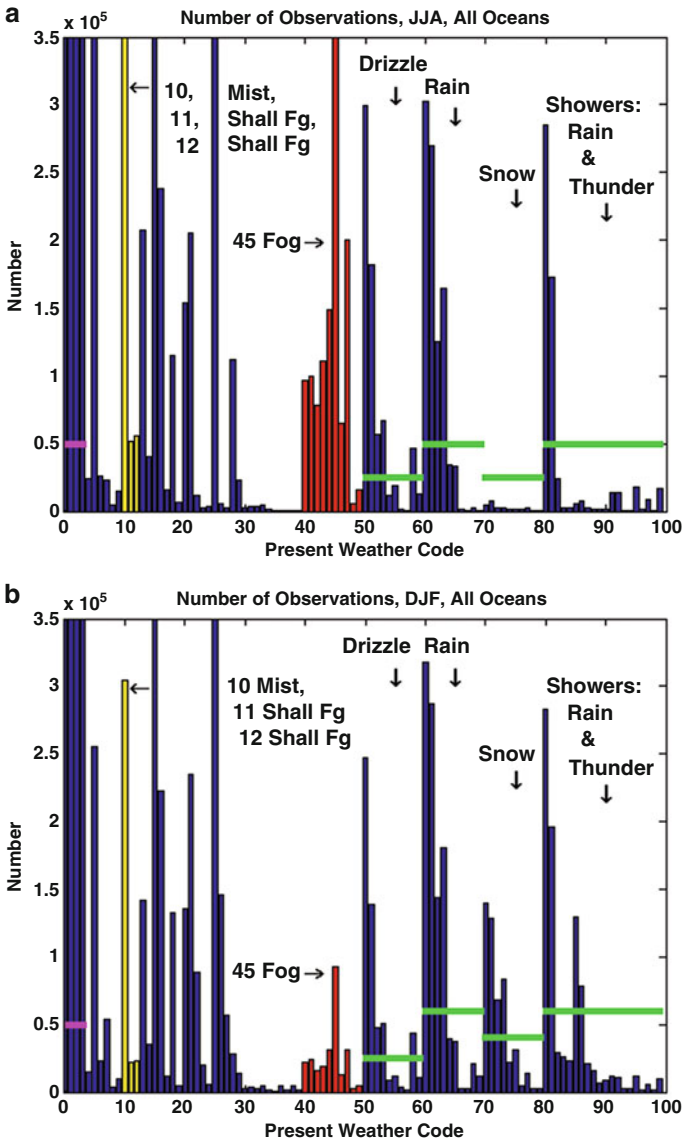

Fig. 2.1 (**a**) June–July–August number of ICOADS present weather observations for the period 1950–2007 over the world oceans. Fog observations, codes 40–49, are red. Yellow bars are for weather somewhat related to, but not fog, and are discussed in the text. Horizontal magenta band marks codes 00–03 which have the four greatest number of observations, make up the majority of the total. Green bands designate weather type blocks that are labeled above with a down arrow. Four weather codes (10, 11, 12, 45) with of special interest (see text) are also labeled. Bars for codes 00–03, 05, 10, 15, 25 and 45, which exceed the upper limit of the graph are cut off at this value. (**b**) December–January–February number of ICOADS present weather observations, 1950–2007, for the world oceans. Bars for codes 00–03, 15 and 25, which exceed the upper limit of the graph, are cut off at this value

drizzle is reduced. Not shown are September, October, and November (SON) or March, April and May (MAM), which have intermediate values between the two seasons shown. A summary is that fog, shallow fog and mist are most frequent during the warm season.

2.6 Zonal and Seasonal Distributions of Present Weather Code Observations

The ww code numbers seem to shift appropriately when concentrating on latitude zone and season. Presented in Fig. 2.2a are different world bands for JJA. Representing the major portions of the world, from tropical to pole are the Tropical band (10 °S to 10 °N), Subtropical band (20 °N to 40 °N), Temperate band (40 °N to 60 °N), and Polar band (>60 °N). Fog is a significant block in the temperate band, which will be shown later to contain the world's two largest fog occurrence maximums that are in the NW Pacific and NW Atlantic, as well as drizzle (50s) and rain (60s). Fog decreases in the subtropical and polar bands and almost disappears in the Tropical band. Snow (70s) is minuscule in the lower three bands, but a small number of occurrences is reported in the polar band. The number of showers (80, 81, 82) is similar in the three lower latitude bands, while the small number of thundershowers (90s) is greatest in the temperate and subtropical bands. The first four codes (00–03) form the bulk of observations in each band.

The present weather observations in the world bands are repeated for DJF (Fig. 2.2b). Fog groups are substantially less in the three northerly bands during DJF, while negligible fog numbers are repeated in the Tropical band. A major shift in DJF is the increased numbers of snow (70s) and showers (80s) in the Polar and Temperate bands. Examination of the present weather observations in other world bands and seasons (not presented) appear as would be expected from the two presented.

2.7 Fog Occurrence Uncertainty

This section investigates the uncertainty of the fog occurrence calculations, the main focus of this chapter. This can be approached different ways although all are essentially related to the standard deviation. As noted in Sect. 2.4, the standard deviation is 8 % for the mean fog occurrence for the world oceans based on the 1950–2007 record. However, the median fog occurrence is very low, 0.2 % which is due to the fact that most of the observations are in temperate and tropical oceans away from coasts where fog is rare (Fig. 2.3).

A special facet to this question is that a stable value for a grid point requires a minimum number of observations. Tests with the smallest number of ship observations needed for a stable estimate suggested that at least 100 observations are

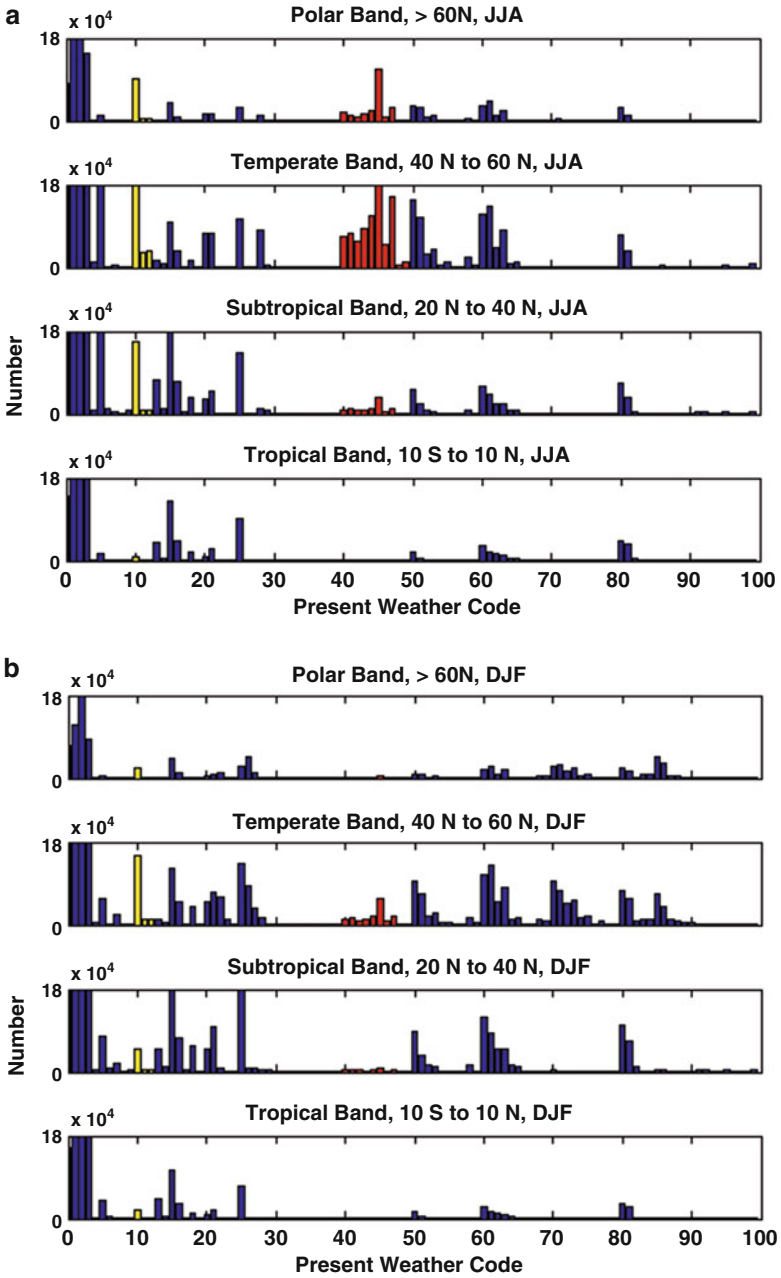

Fig. 2.2 Present weather codes observed in world bands during (**a**) June–July–August and (**b**) December–January–February for 1950–2007. The world bands are Tropical (10°S to 10°N), Subtropical Band (20°N to 40°N) Temperate Band (40°N–60°N) and Polar (>60°N). Bars exceeding the upper limit, such as codes 00–03, 05, 10, and 45 are cut off top at top of graph

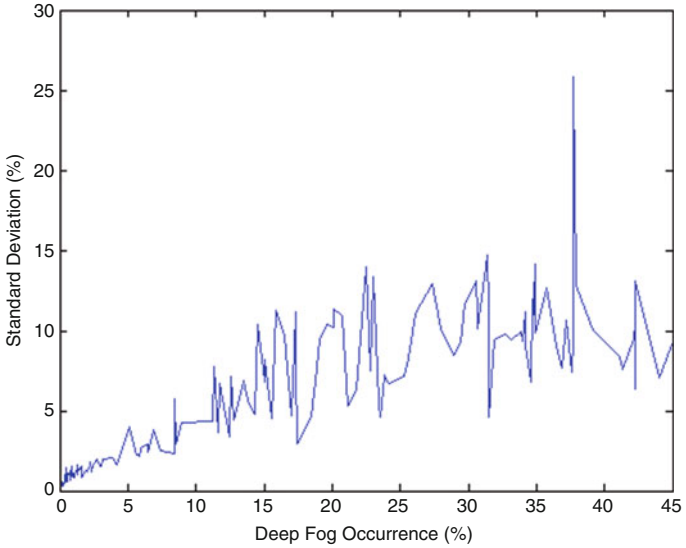

Fig. 2.3 Standard deviation vs. fog occurrence for grid points in the NW Atlantic area 35 °N to 52 °N and 50 °W to 42 °W. For each grid point the June–July–August fog occurrence record is divided into 4-year blocks. The mean for each block is computed and the standard deviation is based upon the 14 4-year blocks for each grid point with in the area

required base an estimate of the fog occurrence over a time period. Major portions of the world oceans do not meet this minimal criteria for a season based on the entire 1950–2007 record. Subdividing the record for climatic trends at a grid point can only be done over heavily traveled shipping lanes in the Northern Hemisphere or combining the observations for multiple grid points.

The effects of high occurrence and number observations on the standard deviation and yearly averaging in a selected portion of the world ocean are now examined. Individual grid point values from 45 °N to 38 °N along 49 °W are shown in Table 2.3 which include high fog occurrence in the northern end and very low in the southern end and all are in major shipping lanes. The mean fog ratio is the average of JJA for single years while the brackets are all JJA values summed together before occurrence is computed. The standard deviation at a grid point for 1 year, 2 year and 4 year averages are presented. There is a strong relationship such that as the mean decreases from high occurrence at higher latitudes to low occurrence at lower latitudes, and the standard deviation systematically decreases for all of the averaging periods. The second is that collecting more observations before making the proportion calculation decreases the standard deviation for all cases.

In the previous paragraph, the effect of yearly averaging is presented. This paragraph shows the relationship of 4-year averages average over an area. At a grid point, for JJA, the record of 1950–2007 is divided into 4 year block for a, total of 14 for each grid point over an area in NW Atlantic 35 °N to 52 °N, 50 °W to 42 °W. This includes high occurrences in the northern portion, (up to 45 %) and very low occurrences (less than 0.2 %) in the southern portion. As the occurrence

Table 2.3 Effect of the JJA fog mean value and the number of years averaged on the standard deviation for grid points along a selected meridian in the NW Atlantic where the mean decreases from high to low with the latitude. See text for further explanation

	Total # all years			Standard deviation (%)		
Grid point position	All ww	Fog	Mean* fog (%)	1 year av	2 years av	4 years av
45N 49W	4494	1939	43.2	14.5	8.7	6.4
44N 49W	5021	2251	45.0	14.7	9.8	7.0
43N 49W	5382	1647	30.6	9.4	6.5	4.6
42N 49W	5161	881	17.0	8.0	5.4	3.0
41N 49W	3901	221	5.6	4.4	3.2	2.2
40N 49W	4463	69	1.5	1.8	1.4	0.8
39N 49W	3450	28	0.8	1.6	1.0	0.9
38N 49W	2340	8	0.3	1.1	0.8	0.5

[a]Value is occurrence mean of 1 year JJA calculations
av, average

decreases from about 17 % to near zero, the standard deviation decreases from 8 % to less than 0.1 %. For fog occurrences of 20–45 %, except for one value, the SD fluctuates ±5 %. Scatter plots of the standard deviation vs. number of observations and fog occurrence vs. number of observation are both without any systematic relationship (not shown).

Another way to view the uncertainty is in comparison between neighboring grid points. The case shown is for fog occurrence at grid points for JJA based on 1950–2007 average. Eight areas were selected to illuminate a range of climate conditions (Table 2.4). These results were computed by pairing each grid point with three neighbors so as to not repeat any: one to the N, one to the NE and one to the East. A vector was generated for the central grid point and a vector for each of the three neighboring grid points. The results are presented in Table 2.4 where statistics are given for the vectors consisting of grid point values for each area. Correlation is between the central vector and the neighboring point vector. The results are consistent with that noted previously – higher occurrences have higher standard deviation. Greatest standard deviation (8–14 %) is in NW ocean fog maximum with highest occurrence. Median values and standard deviations decrease to less than 0.2 % for subtropical and tropical oceans. Correlations between neighboring pairs are greatest in 35 °N to 60 °N latitudes (0.60–0.94 in examples) and are uncorrelated in subtropical and tropical oceans.

Yet another way to view the uncertainty, the difference between neighboring grid point pairs. The set-up is the same as with correlation in previous section and show on the left hand side of Table 2.4. As is expected, the median difference decreases with the decrease in the median occurrence value. The median of 1–4 % in NW oceans falls to less than 0.2 % in subtropical and tropical oceans. The standard deviation of the difference also decreases from a high in NW oceans (~5 %) to less than 0.2 % in subtropical and tropical oceans. A useful result is that any grid point value that differs significantly from its nearest neighbors is suspect.

Table 2.4 Fog occurrence statistics based on the 1950–2007 record at grid points in selected oceanic areas for which the boundaries are shown on the left. GP means "grid points." Pacific Ocean area values are clear while Atlantic Ocean area values are gray shaded. See text for discussion

Area	Grid Points							Difference			
	Num GP's	Num pairs	10%	Med	90%	SD	Corr	10%	Med	90%	SD
NW Ocean – High Fog Occurrence											
43-49N 151-157E	49	147	30.9	43.8	55.6	8.3	0.76	0.7	3.8	9.4	5.5
35-52N 50-42W	162	486	0.2	9.2	35.9	14.2	0.94	0.1	1.3	8.5	4.7
NE Ocean – Moderate to Low Fog Occurrence											
45-50N 134-128W	42	126	3.7	5.6	8.7	1.9	0.63	0.1	0.9	2.3	1.6
45-50N 15-7W	54	162	1.4	2.4	3.6	0.8	0.81	0.1	0.4	0.9	0.5
Subtropical Ocean – Very Low Fog Occurrence											
25-30N 175-165W	66	198	0	0	0.4	0.2	0.16	0	0.2	0.6	0.3
30-35N 40-30W	66	198	0	0.0	0.2	0.1	-0.03	0	0.1	0.2	0.1
Tropical W. Ocean – Very Low Fog Occurrence											
12-17N 110-118E	54	162	0	0.0	0.1	0.1	0.04	0	0.0	0.1	0.1
13-17N 78-68W	55	165	0	0.0	0.1	0.04	0.05	0	0.0	0.1	0.1

3 Worldwide Marine Fog Occurrence

3.1 Mean Quarterly World Ocean Analyses: Number of Observations

The number of present weather observations greater than 100 per one-degree grid point is examined first, as higher numbers give more weight to the results. The number of all present weather observations for JJA is greatest along major shipping routes, with the highest values and no data voids in the northern temperate oceans (Fig. 2.4a). Further, all major shipping routes stand out with their higher numbers, including those in marginal seas such as the Mediterranean Sea and the Red Sea. Away from major shipping routes, there are significant data voids south of 20 °N in the Pacific and south of the Equator in the Atlantic Ocean and Indian Ocean. Most of the ocean south of 35 °S, as well as in the higher Arctic, is without minimum observations. As noted previously, less than 100 observations in a one-degree grid point during a 1950–2007 quarter is considered a data void. The number of observations per degree square is similar in the DJF quarter (Fig. 2.4b), except there are fewer on the edge of the Arctic and somewhat more in the Southern Ocean. The other quarter's numbers are between those of JJA and DJF (not shown).

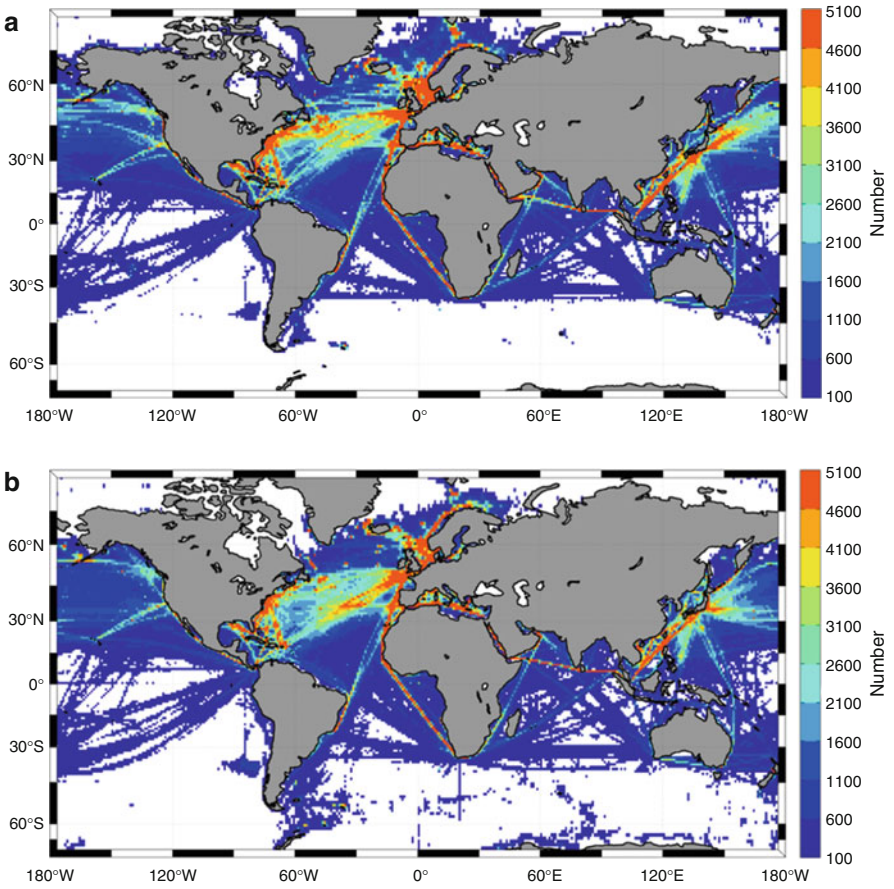

Fig. 2.4 Number of ICOADS present weather observations greater than 100 per 1° grid point for 1950–2007 during (**a**) June–July–August and (**b**) December–January–February

3.2 Mean Quarterly World Ocean Analyses: Fog, Code 40s

The peak worldwide occurrence of marine fog (present weather code 40s) is in JJA, with the greatest values and the largest areas in the NW Pacific and the NW Atlantic (Fig. 2.5a). The NW Pacific maximum to the NE of Japan has the absolute highest values (59.8 %) and with a larger area exceeding that in the NW Atlantic off Labrador, where the peak value is significantly less (45.0 %). Fog occurrence greater than 30 % (half value of the NW Pacific peak) extends from the maximum center to beyond 160 °W, more than half way across the Pacific at this latitude. In contrast, fog occurrence greater than 22 % (half of the NW Atlantic peak) extending eastward from the NW Atlantic maximum does not reach 40 °W, less than one quarter of the distance from the maximum center to Europe. In addition, due to open